Optics Communications 284 (2011) 2007–2011

Contents lists available at ScienceDirect

Optics Communications

journal homepage: www.elsevier.com/locate/optcom

Vector solitons in a laser passively mode-locked by single-wall carbon nanotubes

Jia Haur Wong [a,*], Kan Wu [a], Huan Huan Liu [a], Chunmei Ouyang [a], Honghai Wang [a], Sheel Aditya [a], Ping Shum [a], Songnian Fu [a], E.J.R. Kelleher [b], A. Chernov [c], E.D. Obraztsova [c]

[a] Network Technology Research Centre, School of Electrical and Electronic Engineering, Nanyang Technological University, 50 Nanyang Drive, 637553, Singapore
[b] Femtosecond Optics Group, Physics Department, Imperial College London, London SW7 2AZ, United Kingdom
[c] A.M. Prokhorov General Physics Institute, Russian Academy of Science, 38 Vavilov Street, Moscow 119333, Russia

ARTICLE INFO

Article history:
Received 29 October 2010
Accepted 12 December 2010
Available online 30 December 2010

Keywords:
Single-wall carbon nanotubes
Polarization rotation locking
Vector solitons
Period-doubling
Timing jitter

ABSTRACT

Polarization Rotation Locked Vector Solitons (PRLVSs) are experimentally observed for the first time in a fiber ring laser passively mode-locked by a single-wall carbon nanotube (SWCNT) saturable absorber. Period-doubling of these solitons at certain birefringence values has also been observed. We show that fine adjustment to the intracavity birefringence can swing the PRLVSs from period-doubled to period-one state without simultaneous reduction in the pump strength. The timing jitter for both states has also been measured experimentally and discussed analytically using the theoretical framework provided by the Haus model.

1. Introduction

Temporal solitons in single mode fibers (SMFs) have been widely studied since they were first shown to exist theoretically by Hasegawa and Tappert [1], and later experimentally by Mollenauer [2]. Accelerated by leaps in technology, such as low-loss SMFs, rapid progress has been made and many practicable applications of soliton propagation have emerged. A common feature of SMFs is the presence of birefringence that arises from an imperfect circle core, random mechanical strains and bends, etc. [3,4]. Consequently, SMFs support two orthogonally polarized components because of which the solitons exhibit complex polarization dynamics during propagation. This vector nature of solitons is however ignored in many earlier reports as soliton propagation is mainly treated as a scalar problem that considers only a single polarization component. Due to birefringence in SMFs, the polarization state of solitons will evolve during propagation as the orthogonal polarization components propagate at different group and phase velocities [3,5]. A difference in group velocity between the aforementioned components will cause them to separate temporally, subsequently destroying the solitons. However, Menyuk et al. have shown that, this difference in group velocity can be compensated via a shift in the frequencies of both components, thus enabling solitons to propagate as a single entity [6]. Such vector solitons are known as Group Velocity Locked Vector Solitons (GVLVSs). For vector solitons to propagate without evolution in the polarization state, besides the locking of group velocities, the phase velocities between the orthogonal polarization components have to be locked as well. Referred to as Polarization Locked Vector Solitons (PLVSs), these solitons have their phase velocities locked as a result of the equilibrium between nonlinearity, dispersion in the cavity as well as the balance between gain and loss. Under suitable cavity birefringence, Cundiff et al. reported the observation of such PLVSs in a fiber laser passively mode-locked by Semiconductor Saturable Absorber Mirrors (SESAMs) [7]. Since then, the formation of PLVSs in mode-locked fiber lasers has been widely reported [3,4,7].

As no intracavity polarizing element is required, fiber lasers passively mode-locked by SESAMs have received serious attention for research in vector solitons. Zhao et al. recently reported an observation of vector solitons whose polarization state can rotate and be locked to the cavity roundtrip or at multiples of it [8]. Such vector solitons are referred as Polarization Rotation Locked Vector Solitons (PRLVSs). In this paper, we report an observation of such PRLVSs for the first time in a fiber ring laser passively mode-locked by a single-wall carbon nanotube (SWCNT) saturable absorber which does not require any intracavity polarizing element. Due to the intrinsic dynamic features of the aforementioned fiber laser, period-doubling bifurcation of the PRLVSs is also observed. The period-doubling phenomenon was first presented by Tamura et al. in a soliton fiber laser [9]. Later, Soto-Crespo et al. presented the existence of period-one and period-doubling phenomena in a passively mode-locked fiber laser [10]. More recently, period-doubling route to multi-pulse formation was reported by Ilday et al. in a fiber laser [11]. Soliton propagation however is treated as a scalar phenomenon in these reports. Further, Zhao et al. have demonstrated experimentally the existence of period-doubled PLVSs in

* Corresponding author. Tel.: +65 67904527.
E-mail address: wong0779@ntu.edu.sg (J.H. Wong).

0030-4018/$ – see front matter
doi:10.1016/j.optcom.2010.12.048

a fiber laser passively mode-locked by SESAMs [12]. Period-doubling is considered to be a form of instability as the pulse train acquires additional frequency components. It is observed that this instability can itself be stable as both the pulse shape and energy change periodically between adjacent pulses. However, such pulse-to-pulse non-uniformity is still considered to be detrimental for its use in various applications, and should be avoided. For period-doubling phenomenon in fiber lasers based on SESAMs, it was observed that the solitons could swing from period-doubled state to period-one state through adjustment to the cavity birefringence accompanied by reduction in pump strength [12,13]. In contrast, for the fiber laser based on a SWCNT saturable absorber we experimentally observe that period-one state of PRLVSs can be attained by sole adjustment of the cavity birefringence, without compromising the pump strength. Besides the instability induced by period-doubling, consideration of timing jitter noise is also significant as the noise performance of the mode-locked laser is relevant for many applications. Thus, the timing jitter noise of the PRLVSs for both period-doubled and period-one state is also examined in this paper. We experimentally observe an insignificant difference in the timing jitter between the aforementioned states of the PRLVSs. The reason for this insignificant difference is discussed in the paper.

2. Experimental setup

The fiber laser used in the experiment is schematically shown in Fig. 1. It has a ring configuration and is mode-locked by a SWCNT saturable absorber. With a total fiber length of 5.38 m, the fiber laser has a fundamental repetition rate of 37.17 MHz. The gain medium is a 0.25 m long erbium-doped fiber (LIEKI Er110) with group velocity dispersion (GVD) 0.012 ps^2/m. A wavelength-division multiplexer (WDM) which comprises 1 m HI1060 pigtailed fiber with GVD +0.020 ps^2/m, is also included. The single mode fibers (SMF28) that make up the rest of the ring cavity have a total length of 4.13 m with GVD −0.022 ps^2/m. The total net cavity dispersion is −0.068 ps^2 at 1550 nm. Unidirectional operation is ensured with the use of an optical isolator, while light is coupled out of the cavity via a 90/10 fiber coupler. A fiber-based polarization controller (PC) is included to adjust the cavity birefringence and optimize the mode-locking condition. The SWCNTs used are embedded between carboximethyl cellulose (CMC) films, allowing low self starting pump power and high damage threshold [14]. An optical spectrum analyzer (Ando AQ-6315B) and a signal source analyzer (SSA, Rohde & Schwarz FSUP26) as well as a 350 MHz oscilloscope (Agilent 54641A) are used to monitor the laser output. A commercial autocorrelator (Femtochrome FR-103MN) is used to measure the temporal pulse width.

3. Experimental results

As pump driven current increases to above 200 mA, the fiber laser shown in Fig. 1 self-starts. It is observed that the fiber laser operates in a single-pulse mode at this pump strength. On the other hand, most fiber lasers based on SESAMs would operate in multi-pulse mode at self-starting pump strength. At certain settings of cavity birefringence, intensity period-doubling of the temporal pulse train is observed. This is evident from the periodic intensity difference between adjacent pulses in Fig. 2(a). Similar to the scalar cases, this period-doubling phenomenon of the vector solitons is due to the intrinsic dynamic feature of the fiber laser itself. A basic characteristic of period-doubling state is the appearance of relatively weak frequency components positioned at half of the fundamental repetition frequency in the RF spectrum as shown in Fig. 2(d). To assess the individual characteristics of the vector solitons' orthogonal polarization components, a polarizer is placed before the photodetector. Orientating the polarizer to receive maximum transmission at the photodetector, the length of the long

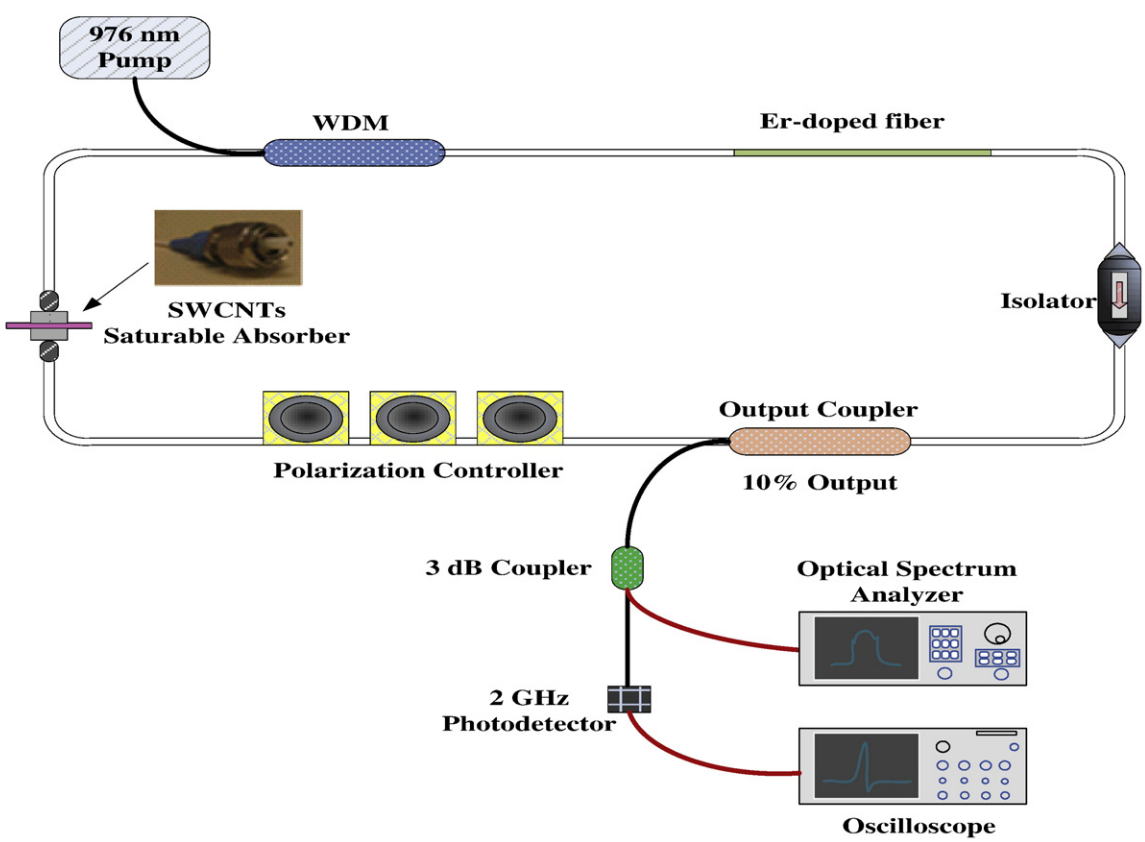

Fig. 1. Schematic configuration of fiber laser passively mode-locked by SWCNTs.

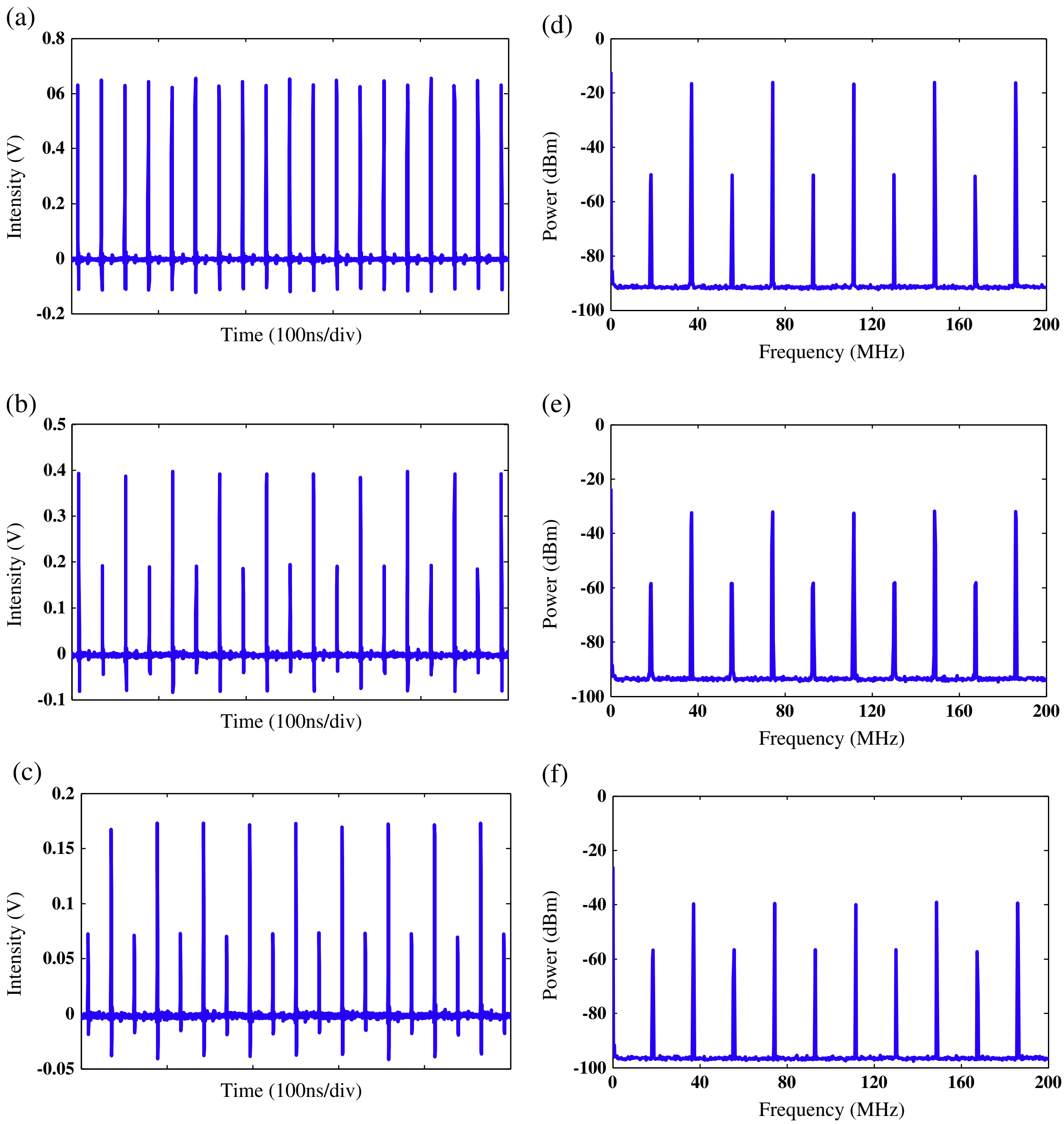

Fig. 2. Oscilloscope trace and RF spectrum of the vector solitons. (a) Pulse-train for the vector solitons without an external polarizer; (b) pulse-train for the polarization along the long axis of vector solitons; (c) pulse-train for the polarization along the short axis of the vector solitons; and (d–f) corresponding RF spectra of the vector solitons.

axis of the polarization ellipse can be determined. Likewise, the length of the short axis is determined with a further 90° rotation of the polarizer's orientation. Fig. 2(b) and (c) shows the intensity along the long and short axes of the polarization ellipse, respectively. We observe a larger periodic variation in the temporal pulse intensity in both axes as compared to Fig. 2(a). Clearly, both axes exemplify polarization states which rotate and are locked to twice the roundtrip time, verifying the existence of PRLVSs in the cavity. Corresponding to the period-doubling, there exist weak frequency components in the RF spectrum for both axes of the PRLVSs as shown in Fig. 2(e) and (f).

Fig. 3(a) shows the measured optical spectra of the period-doubled PRLVSs. Extra sets of soliton sidebands are observed to exist apart from the well-known Kelly soliton sidebands. Different from the Kelly sidebands, the positions of these extra sidebands are very sensitive to the intracavity polarization controller's orientation. At the position of these extra sidebands, a pronounced peak is observed for one of the orthogonal polarization component, while a dip is observed for the other component. These observations indicate that these extra sidebands form due to the coherent energy exchange between the two orthogonal polarization components [15]. Examining the energy exchange between the axes further, it appears that there is no preferred direction of energy flow. Specifically, energy can flow from the strong component to the weak, or vice versa.

Significantly, we observe that these vector solitons can swing from period-doubled to period-one state by fine adjustment to the cavity birefringence while keeping other parameters unchanged. Unlike most fiber lasers based on SESAMs that have been reported in the literature, in the present case period-one state is achieved without reducing the pump strength. Obviously, the weak frequency components which are a characteristic feature of period-doubling bifurcation

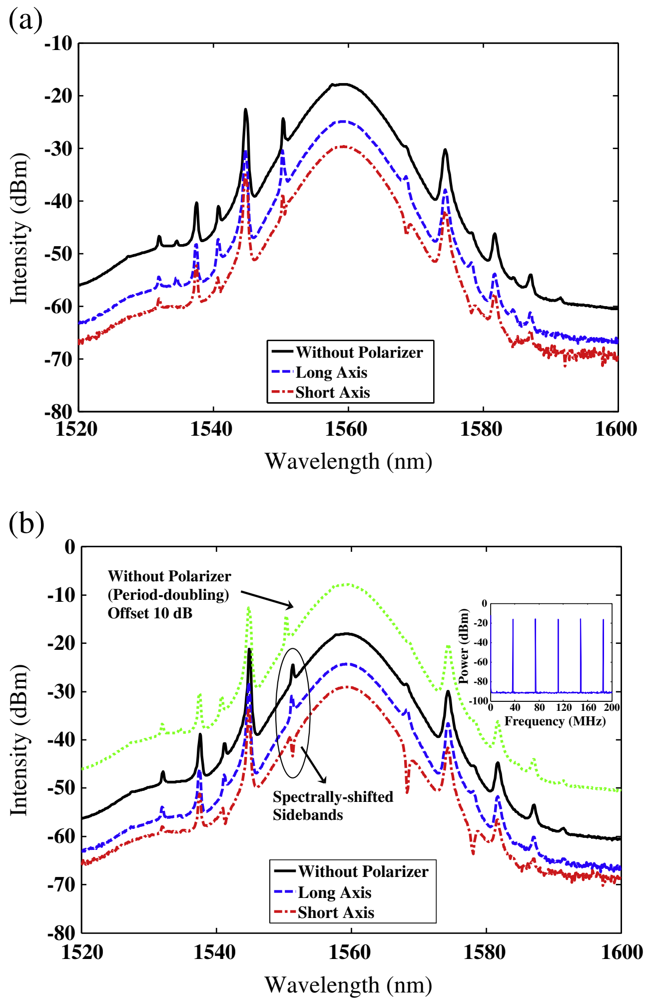

Fig. 3. Output optical spectra for, (a) period-doubling state vector solitons, and (b) period-one state vector solitons.

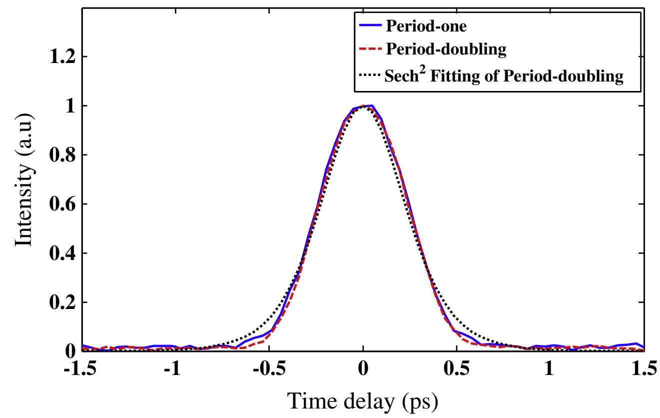

Fig. 4. Autocorrelation traces of period-one and period-doubling state vector solitons.

are suppressed in the RF spectrum for period-one state as illustrated by the inset in Fig. 3(b). Examining the pulse train for the orthogonally polarized components again, the periodic variation in the intensity of the temporal solitons further confirms that the period-one solitons are PRLVSs. Coherent energy exchange is still observed between the orthogonal polarization components for period-one state PRLVSs as shown in Fig. 3(b). In addition, a shift in the spectral position of the extra sidebands is also observed. This happens because the positions of these extra sidebands are cavity birefringence dependent.

Since the pump strength remains unchanged as period-doubling state swings to period-one, there is insignificant change in the measured pulse duration and pulse energy. As shown in Fig. 4, the pulse durations measured are 534fs and 524fs for period-one and period-doubling state, respectively. The average pulse powers measured are 621 μW and 614 μW for period-one and period-doubling state, respectively.

4. Measurement of timing jitter noise

The timing jitter noise for both period-doubling and period-one states has also been investigated. Here, root mean square (rms) timing jitter is calculated based on the following relation [16]:

$$\Delta t_{rms} = \frac{1}{2\pi n f_{rep}}\sqrt{2\int_{f_L}^{f_H} S_n(f)df} \tag{1}$$

where n denotes the harmonic order of the carrier measured, f_{rep} is the fundamental repetition frequency, and $S_n(f)$ is the measured power spectral density (PSD) around the nth harmonic. The rms timing jitter is calculated over a frequency offset range between f_H and f_L at the 4th harmonic (~148.68 MHz) using the above relation.

Fig. 5 presents the measured phase noise spectrum for both period-one and period-doubling states between the 10 Hz to 3 MHz frequency offset range. The phase noise spectrum is measured by the signal source analyzer (SSA, Rohde & Schwarz FSUP26). The rms timing jitter for period-one and period-doubling states is calculated to be 605 fs and 645 fs, respectively and can be considered to be equal within the measurement errors. This equality in the timing jitter noise can be explained in accordance with Haus' model [16]. This well-known model defines the spectrum of timing jitter induced by quantum noise in a mode-locked laser by the following equation [16]:

$$S_t(f) = \frac{4D^2}{T_{rt}^2}\frac{D_p}{(2\pi f)^2\left((2\pi f)^2 + \tau_p^{-2}\right)} + \frac{D_t}{(2\pi f)^2}. \tag{2}$$

This model identifies two different influences of quantum noise on timing jitter, with the first term from (1) being an indirect influence while the second term is a direct influence. $D_p = \frac{2}{3\omega_0\tau^2}\theta\frac{2g}{T_{rt}}h\nu$ and $D_t = \frac{\pi^2\tau^2}{6\omega_0}\theta\frac{2g}{T_{rt}}h\nu$ are the diffusion constants of quantum noise representing the noise properties of offset frequency and timing respectively, θ is the enhancement factor due to incomplete inversion of the gain medium, $\tau_p = \frac{3\pi^2 T_{rt}\Delta f_g^2\tau^2}{2g}$ is the relaxation time, D is half of the total group velocity dispersion, T_{rt} is the roundtrip time, ω_0 is the pulse energy in the cavity, τ is the pulse duration, g is the incremental gain per roundtrip, and Δf_g is the gain bandwidth. The corresponding phase noise spectrum is expressed as $S_p(f) = (2\pi f)^2 S_t(f)$. Since there

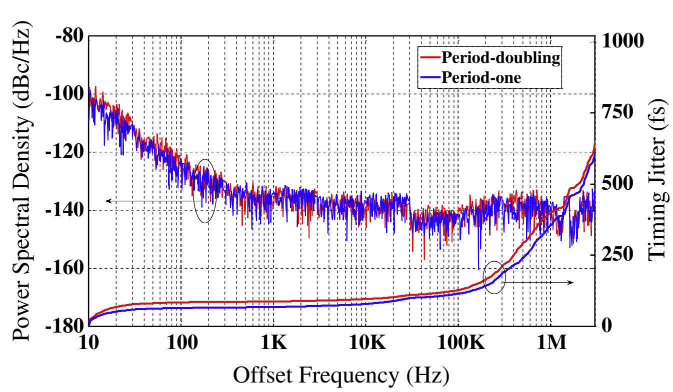

Fig. 5. Phase noise and integrated timing jitter for period-one and period-doubling state vector solitons.

is little difference in the pulse energy and duration for both period-one and period-doubling state, it is easy to understand from the mathematical expressions that there is also little difference in the timing jitter as shown in the experimental and analytical results. This is in contrast to the fiber lasers based on SESAMs where a significant difference in the pulse energy due to the change in the pump strength results as period-doubling state swings to period-one state; this leads to a significant difference in timing jitter noise as well [13].

5. Conclusion

In this paper, we have reported the first observation of PRLVSs in a fiber laser passively mode-locked by a SWCNT saturable absorber. For certain settings of cavity birefringence, period-doubling of the PRLVSs is evident. It is demonstrated that the period-doubled PRLVSs can swing to period-one state requiring only adjustment to the cavity birefringence and no reduction in pump strength. We measured the pulse duration and energy and found little or no difference between the PRLVSs in both states. Subsequently, the timing jitter noise for both cases was also measured experimentally as well as discussed analytically and, as expected, insignificant difference was observed.

References

[1] A. Hasegawa, F. Tappert, Applied Physics Letters 23 (1973) 142.
[2] L.F. Mollenauer, R.H. Stolen, J.P. Gordon, Physical Review Letters 45 (1980) 1095.
[3] S.T. Cundiff, B.C. Collings, N.N. Akhmediev, J.M. Soto-Crespo, K. Bergman, W.H. Knox, Physical Review Letters 82 (1999) 3988.
[4] B.C. Collings, S.T. Cundiff, N.N. Akhmediev, T.M. Soto-Crespo, K. Bergman, W.H. Knox, Journal of the Optical Society of America B (Optical Physics) 17 (2000) 354.
[5] J.M. Soto-Crespo, N.N. Akhmediev, B.C. Collings, S.T. Cundiff, K. Bergman, W.H. Knox, Journal of the Optical Society of America B (Optical Physics) 17 (2000) 366.
[6] C.R. Menyuk, Journal of the Optical Society of America B (Optical Physics) 5 (1988) 392.
[7] S.T. Cundiff, B.C. Collings, W.H. Knox, Optics Express 1 (1997).
[8] L.M. Zhao, D.Y. Tang, H. Zhang, X. Wu, Optics Express 16 (2008) 10053.
[9] K. Tamura, C.R. Doerr, H.A. Haus, E.P. Ippen, IEEE Photonics Technology Letters 6 (1994) 697.
[10] J.M. Soto-Crespo, M. Grapinet, P. Grelu, N. Akhmediev, Physical Review E (Statistical, Nonlinear, and Soft Matter Physics) 70 (2004) 66612.
[11] F.O. Ilday, J. Buckley, F.W. Wise, Conference on Lasers and Electro-Optics (CLEO), 16-21 May 2004, IEEE, Piscataway, NJ, USA, 2004, pp. 2 pp. vol.1, 2004.
[12] L.M. Zhao, D.Y. Tang, H. Zhang, X. Wu, C. Lu, H.Y. Tam, Optics Communications 281 (2008) 5614.
[13] C. Ouyang, H. Wang, P. Shum, S. Fu, J.H. Wong, K. Wu, Desmond Rodney C.S. Lim, Vincent K.H. Wong, Kenneth E.K. Lee, Optics Communications 284 (2011) 619.
[14] A.V. Tausenev, E.D. Obraztsova, A.S. Lobach, A.I. Chernov, V.I. Konov, P.G. Kryukov, A.V. Konyashchenko, E.M. Dianov, Applied Physics Letters 92 (2008) 171113.
[15] H. Zhang, D.Y. Tang, L.M. Zhao, N. Xiang, Optics Express 16 (2008) 12618.
[16] H.A. Haus, A. Mecozzi, IEEE Journal of Quantum Electronics 29 (1993) 983.